Supporting Information

Biomass-based 0D/3D N-CQD/MIL-53(Fe) photocatalyst for simultaneous remediation of multiple hazardous pollutants in sewage

Taotao Qiang[a,b]*, Lu Chen[a,b], Xiangtao Qin[a,b]

Supplementary Section 1:

1. Preparation and activation

1.1. The synthesis of P-N-CQD/MIL-53(Fe)

P-N-CQD:

The discarded sycamore leaves were dried in an oven at 70 ℃ for 24 h, and then completely grounded into powder. The sycamore leaves powder (1.0 g) was dissolved in deionized water (50 mL), 0.2 g of urea was added after that, and stirred for 30 min until the urea was completely dissolved. Transferred the above solution into a Teflon-lined autoclave (100 mL) sealed in stainless steel tank, and heated for 18 h (180 ℃). Then, the crude N-CQD could be received after cooling the above system to room temperature. The prepared samples were filtered with 9mm filter paper and dialyzed with 500 molecular weight dialysis bags for three days with water changing every 3 hours. The pure solid P-N-CQD was obtained by freeze-drying for 24 hours at last.

P-N-CQD/MIL-53(Fe):

P-N-CQD/MIL-53(Fe) was prepared by in-situ synthesis. $FeCl_3$•$6H_2O$ (0.8 g) and 0.4 g of H_2BDC were dissolved in DMF (65 mL), kept stirring (30 min) for fully

dissolving, then added a certain amount of P-N-CQD, continued magnetic stirring until the solvent turned from transparent into dark yellow. The above solution was then transferred to a 100 mL Teflon-lined autoclave, and heated at 150 °C for 10 hours, the resulting yellow powder was dispersed in ethanol for activation after cooling to room temperature.

1.2. The activation methods

In the synthesis of MOFs materials, the activation mode is of great important. In this research, two activation methods were used for comparison:

(1) After centrifugal filtration, the obtained P-N-CQD/MIL-53(Fe) was soaked in ethanol for two days, and the ethanol was changed every 5 hours. Finally, the obtained yellow powder was dried in a vacuum drying oven at 70 ℃ for 3 days, and the dried P-N-CQD/MIL-53 (Fe) was put into the sample tube for further testing.

(2) The activation temperature was adjusted in the second method of activating. The resulting P-N-CQD/MIL-53(Fe) was dispersed in ethanol firstly, and then transferred to a three-mouth flask, and the boiling point of ethanol was reached through an oil bath at 90 ℃. So that the DMF remaining in the samples could be completely removed.

2. Characterization

2.1. Reagents

Ferric chloride hexahydrate ($FeCl_3$•$6H_2O$) (A.R.), urea (A.R.), diphenyl carbonyl hydrazine (A.R.), terephthalic acid (99%), concentrated sulfuric acid (98.0%),

phosphoric acid (A.R.), N, N-dimethylformamide (DMF) (A.R.), potassium dichromate (A.R.), acetone (A.R.), methyl alcohol (A.R.), hydrochloric acid (38%). The above reagents utilized in our study were purchased from Aladdin Chemical. The water used during the experiment was deionized by the laboratory water purify system.

2.2. Characterization techniques

The chemical structure of as-prepared samples was analyzed by Fourier transform infrared (FTIR) spectrometer (Bruker Alpha VECTOR-22, Germany) using KBr as the reference at room temperature. The crystalline phase and spatial structure of the above samples were portrayed by XRD diffractometer (Bruker D8-Advance, with Cu Kα radiation (λ=1.54 Å)) and Raman spectroscopy (Renishaw-invia spectrometer (λ=532 nm)). X-ray photoelectron spectrometer (XPS, AXIS SUPRA instrument, UK) was carried out to obtain the chemical configuration of samples, the standard C 1s peak (284.6 eV) was used as the internal standard. The morphology of above composites was investigated by Hitachi S-4800 field emission field emission scanning electron microscope (FE-SEM, Hitachi S-4800). Transmission electron microscopy (TEM, FEI Tecnai G2 F20S-TWINFEI, the accelerating voltage: 200 KV) was carried out to exhibit the microstructure and other details of the as-synthesized samples. Furthermore, the relevant surface areas and pore distributions information of the above samples were calculated using Brunauer-Emmett-Teller (BET) method and nitrogen adsorption-desorption analysis (ASAP2420 USA). Electron spin resonance (ESR, JEOL JES-FA200) was used to analyze the free radical species that play major roles in the reaction.

The photochemical properties were analyzed through UV-vis near-infrared spectrophotometer at wavelengths of 200-800 nm (Carry 5000, USA) using $BaSO_4$ as the reference. And the photoluminescence (PL) spectrum was obtained by fluorescence spectrometer (FS5, Edinburgh) at an excitation wavelength of 320 nm. Inductively Coupled Plasma Optic Emission Spectroscopy (ICP-OES) (Aglient 5110) was used to test the content variation of metal ions in composites to verify the safety and stability of catalysts. The concentration of total organic carbon (TOC) was determined by a TOC auto analyzer (Liqui TOC II).

2.3. Electrochemical detection

To investigate the photoelectrochemical (PEC) properties, electrochemical test was performed on the electrochemical workstation (PARSTAT 4000). Electrochemical impedance spectroscopy (EIS), photocurrent response curves (I-t) and Mott-Schottky plots were tested. A three-electrode system was established with Na_2SO_4 solution (0.5 M) as the electrolyte, Platinum (Pt) electrode, ITO glass, and Ag^+/AgCl electrode as the counter electrode, working electrode and reference electrode, respectively. Samples of the same mass were ultrasonically dispersed in an equivalent ethanol containing a small amount of nafion, and the dispersion was evenly coated on the conductive surface of ITO glass. The coated ITO glass was regarded as the working electrode after dried at room temperature.

Supplementary Section 2: Figures and tables

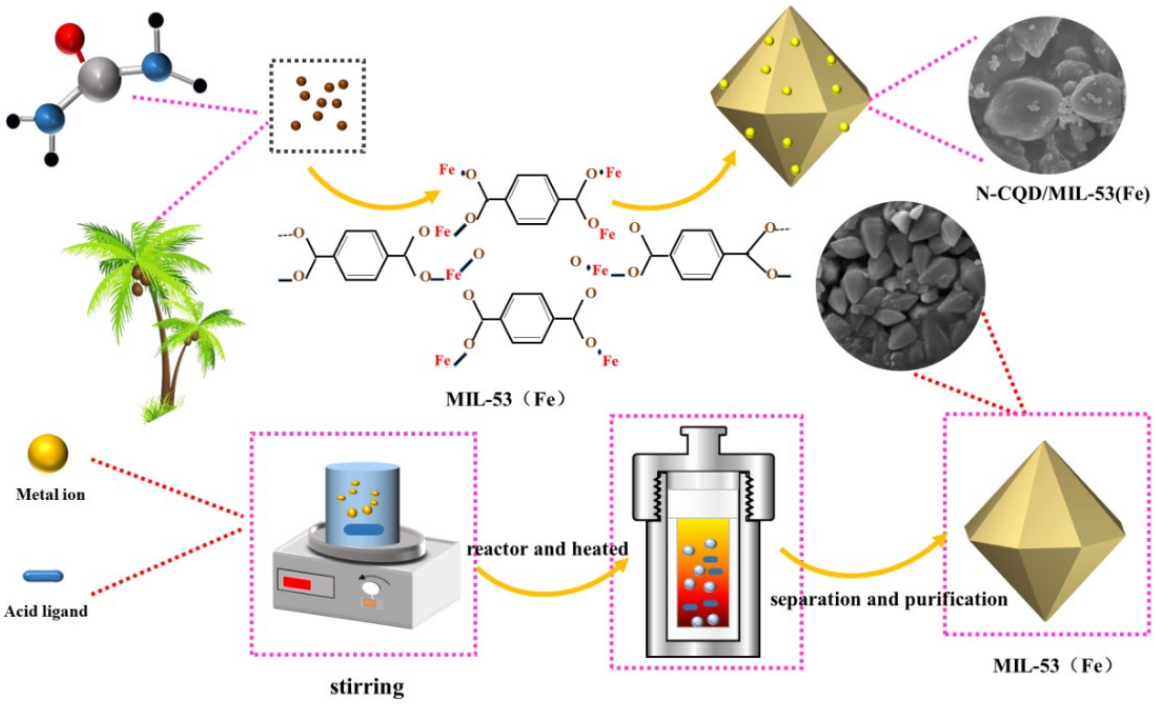

Fig.S1 Schematic diagram of N-CQD/MIL-53(Fe) preparation

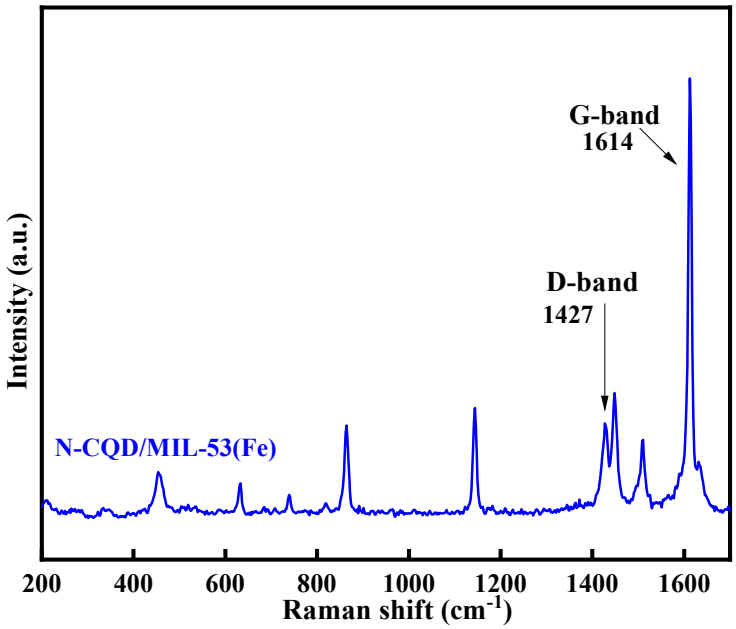

Fig.S2 Raman spectra of N-CQD/MIL-53(Fe) composite

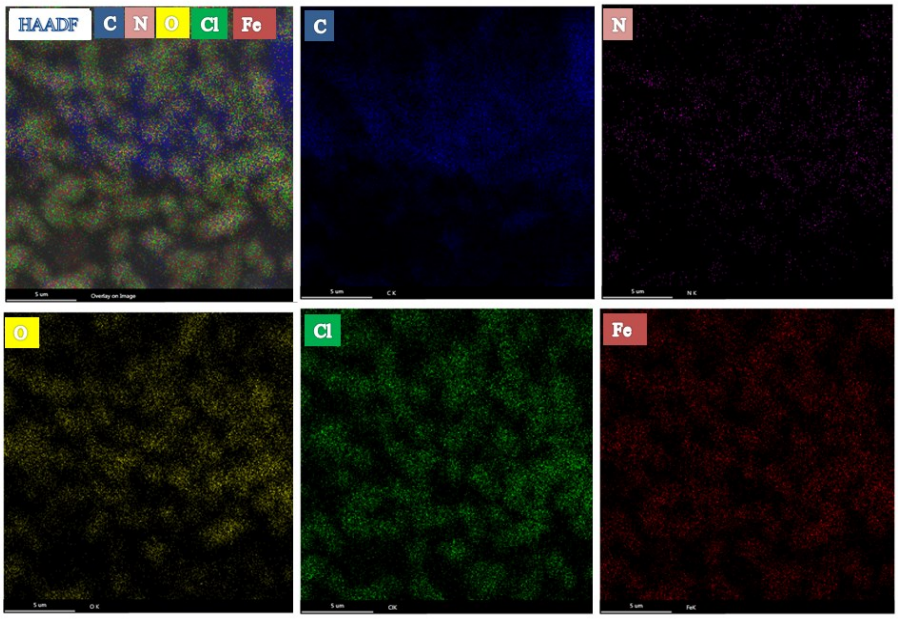

Fig.S3 EDX element mapping of N-CQD/MIL-53(Fe)

Tab.S1 Orthogonal experiments of MIL-53(Fe) preparation

number	Temperature (℃)	Time (h)	Ratio
1	130	20	2：1
2	130	22	8：5
3	130	24	4：3
4	150	20	8：5
5	150	22	4：3
6	150	24	2：1
7	170	20	4：3
8	170	22	2：1
9	170	24	8：5

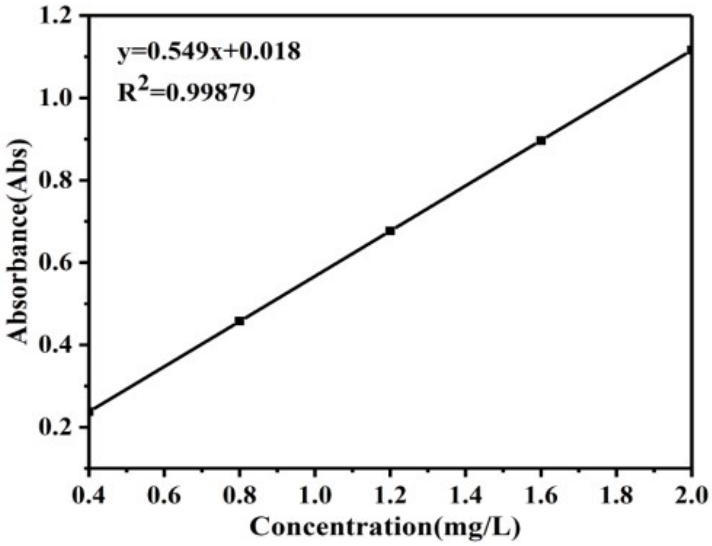

Fig.S4 Standard curve for hexavalent chromium solution

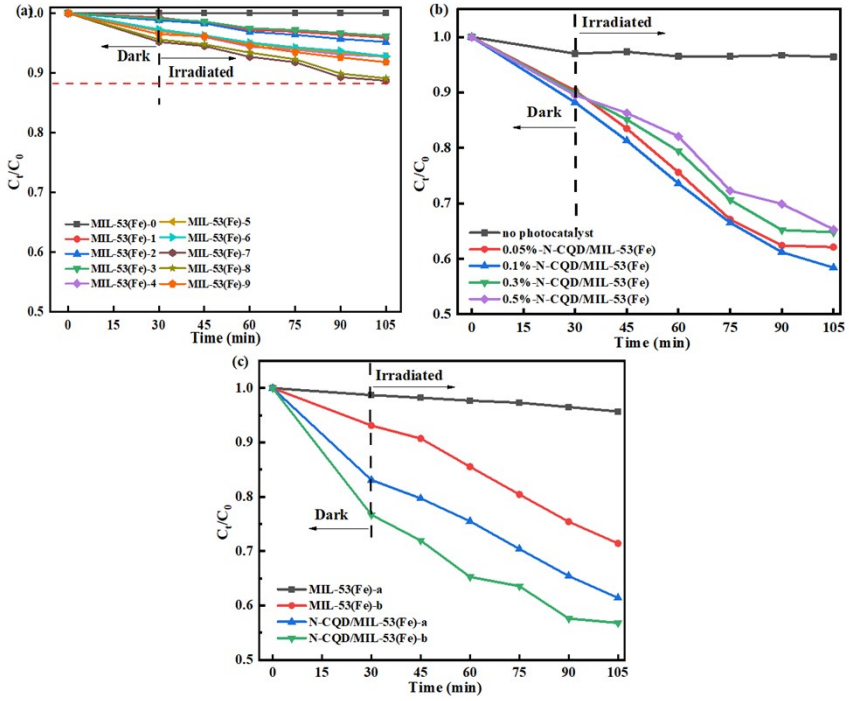

Fig.S5 The effect of MIL-53(Fe) preparation (a); N-CQD loading rate (b); and the activation temperature (c) on the photocatalytic reduction ability of Cr (VI)

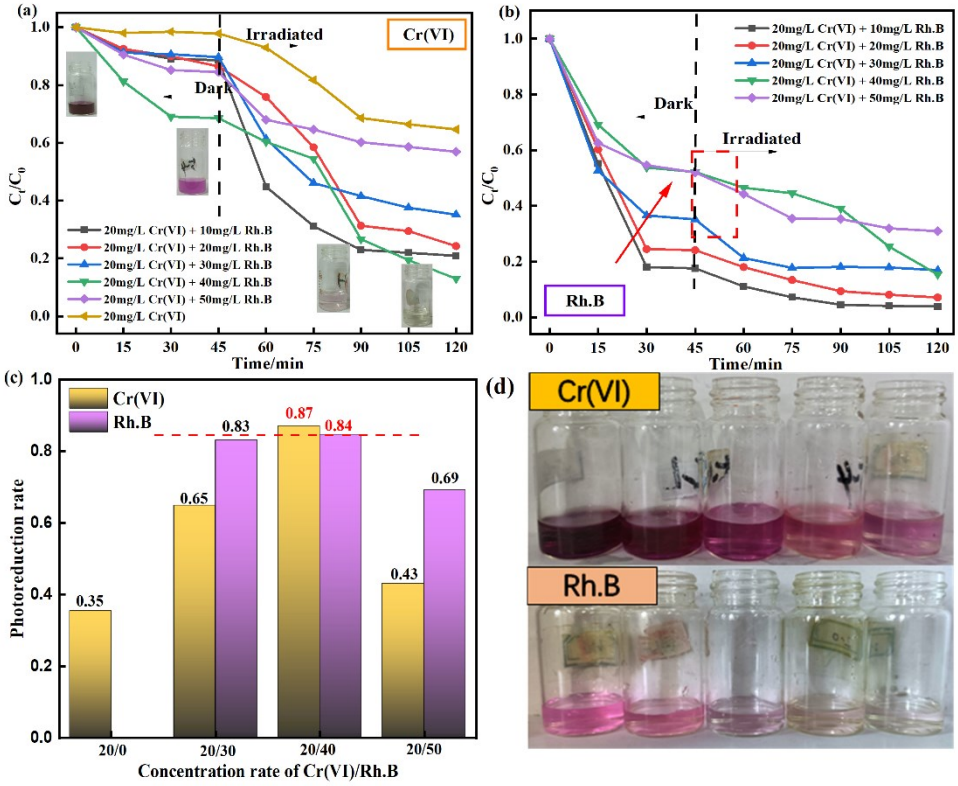

Fig.S6 The concentration variation of Cr (VI) (a); Rh.B (b); and photocatalytic reduction rate (c) of N-CQD/MIL-53(Fe); real time images of photocatalytic experiments (d)

In the experiment, we found that Rh.B was easily adsorbed in the dark experiment, caused too low the concentration to be reacted when turned on the light. Therefore, we reduced the amount of catalysts from 20 mg to10 mg and increased the concentration range of Rh.B to 10 to 50 mg/L, the relevant results were shown as Fig.S6. As it can be seen in Fig.S6 (a), the photoreduction rate of Cr (VI) without Rh.B was not ideal, which draws quite the same conclusion as the system of Cr (VI) and MB. When Rh.B was put in as hole scavenger, all reduction rates of Cr (VI) were better than that of a single system. Intriguingly, when the Rh.B concentration was 40 mg/L, the Cr (VI) reduction was achieved most completely. Fig.S6 (b) illustrated the Rh.B degradation rate in the bi-system. As we expected, when the Rh.B concentration was too low (10 and 20 mg/L), the adsorption effect was too large to evaluate the photocatalytic effect correctly, by virtue of the dye was almost removed from the aqueous. Consider the above situation, we chose the case when the concentration of Rh.B was above 30 mg/L (pointed by the red arrow) to examine the ability of catalyst.

It can be found that the degradation of Rh.B was also very satisfactory when the concentration reached to 40 mg/L. In short, in the bi-component sewage system of Cr (VI) (20 mg/L) and Rh.B (40 mg/L), the photocatalyst N-CQD/MIL-53(Fe) exhibits the same excellent performance as other dye systems, in which, the photoreduction rate of Cr (VI) reached 87 %, which is more than 2 times higher than the single system, and the photodegradation rate of Rh.B reached 84 % at the same time.

Tab.S2 The removed efficiency of different catalysts in bi-component system

Catalyst	***System***	***Removed efficiency (%)***	***Refrence***
MIL-53(Fe)/CQDs/2%Au	Cr(VI) and MG	40.2/100.0	[1]
	Cr(VI) and Rh.B	69.2/98.1	
WO_3/MIL-53(Fe)	Cr(VI) and MB	72.5/87.4	[2]
	Cr(VI) and 2,4-D	80.8/ 90.5	
MIL-53(Fe)	Cr(VI) and MG	71/100	[3]
	Cr(VI) and Rh.B	69/84	
MIL-101(Fe)/g-C3N4	Cr(VI) and bisphenol A	68/94.8	[4]
MIL-68(Fe)	Cr(VI) and MG	80.3/94.5	[5]
AgI/$BiVO_4$	Cr(VI) and TC	69/88	[6]
mesoporous $BiVO_4$	Cr(VI) and MB	97/95 **(pH= 1.5)**	[7]
Fe(III)-$K_2Ti_6O_{13}$	Cr(VI) and MB	80/83	[8]

$SrTiO_3$/($BiFeO_3$ @ZnS)	Cr(VI) and 2,4-D	91/97 **(pH= 2.1)**	[9]
N-CQD/MIL-53(Fe)	**Cr(VI) and MB**	**90.13/69.31 (pH= 6.8)**	**our work**
	Cr(VI) and Rh.B	**87.02/84.61 (pH= 6.8)**	**our work**

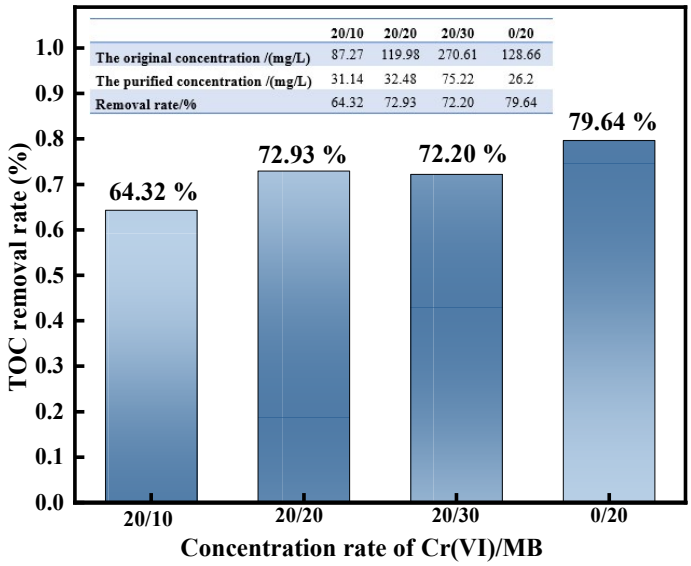

Fig.S7 TOC mineralization after irradiation in the binary systems

Tab.S3 ICP-OES results of Fe (III) content in the original sample and the recycled sample after using 5 times

Iron	The content of Fe (III)/(mg/L)		
	MIL-53(Fe)	N-CQD/MIL-53(Fe)	Recycled N-CQD/MIL-53(Fe)
Fe 2382	0.4783	0.7109	0.575
Fe 2395	0.4535	0.6753	0.5426
Fe 2599	0.4958	0.6324	0.5925
Total	1.4276	2.0102	1.7101

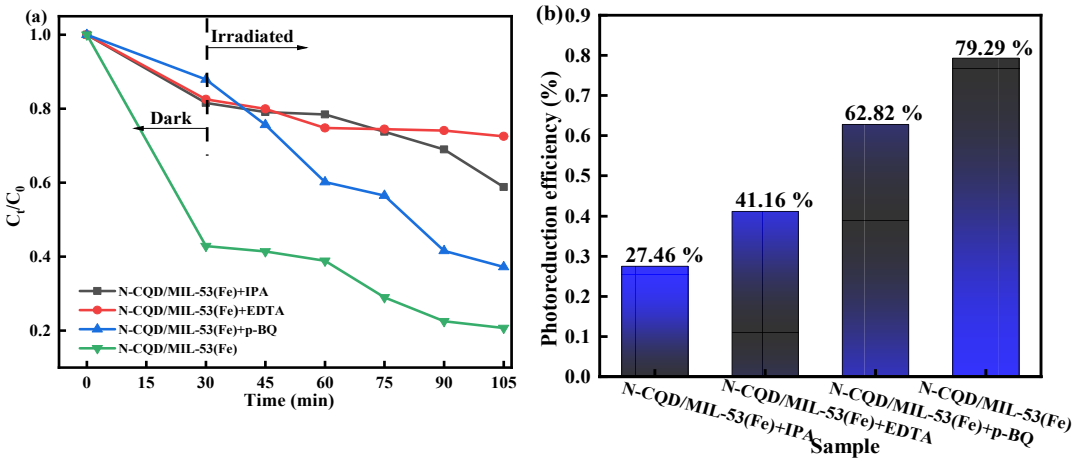

Fig.S8 The free radical trapping experiments of N-CQD/MIL-53(Fe)

1. M. Wang, G. Tan, D. Zhang, B. Li, L. Lv, Y. Wang, H. Ren, X. Zhang, A. Xia and Y. Liu, *Applied Catalysis B: Environmental*, 2019, **254**, 98-112.
2. A. A. Oladipo, *Process Safety and Environmental Protection*, 2018, **116**, 413-423.
3. R. Liang, F. Jing, L. Shen, N. Qin and L. Wu, *Journal of Hazardous Materials*, 2015, **287**, 364-372.
4. F. Zhao, Y. Liu, S. B. Hammouda, B. Doshi, N. Guijarro, X. Min, C.-J. Tang, M. Sillanpää, K. Sivula and S. Wang, *Applied Catalysis B: Environmental*, 2020, **272**, 119033.
5. F. Jing, R. Liang, J. Xiong, R. Chen, S. Zhang, Y. Li and L. Wu, *Applied Catalysis B: Environmental*, 2017, **206**, 9-15.
6. W. Zhao, J. Li, B. Dai, Z. Cheng, J. Xu, K. Ma, L. Zhang, N. Sheng, G. Mao, H. Wu, K. Wei and D. Y. C. Leung, *Chemical Engineering Journal*, 2019, **369**, 716-725.
7. G. Xie, H. Wang, Y. Zhou, Y. Du, C. Liang, L. Long, K. Lai, W. Li, X. Tan, Q. Jin, G. Qiu, D. Zhou, H. Huo, X. Hu and X. Xu, *Journal of the Taiwan Institute of Chemical Engineers*, 2020, **112**, 357-365.
8. A. Khan, U. Alam, D. Ali and M. Muneer, *ChemistrySelect*, 2018.
9. Z. Qu, Z. Liu, A. Wu, C. Piao, S. Li, J. Wang and Y. Song, *Separation and Purification Technology*, 2020, **240**, 116653.